ELSEVIER

Thermochimica Acta 356 (2000) 133–138

thermochimica acta

www.elsevier.com/locate/tca

A new method for determining solute diffusivity in polymers from data obtained by non-isothermal thermogravimetry

G. Karlsson, M.S. Hedenqvist, U.W. Gedde*

Department of Polymer Technology, Royal Institute of Technology, UWG, SE-100 44 Stockholm, Sweden

Received 16 September 1999; accepted 16 February 2000

Abstract

A numerical method for determining solute diffusivity in polymers over wide temperature ranges was developed based on non-isothermal thermogravimetry (TG). The method combines the Fickian equations with a heat transfer equation in order to take into account temperature gradients within the polymer sample during a heating scan. The requirement of thermal equilibrium in the specimen during the heating scan need not be fulfilled, and this permits the study of desorption of solute from thick specimens at high heating rates. The numerical procedure is capable of considering concentration-dependent solute diffusivity and temperature-dependent thermal diffusivity. The method was tested on the desorption of *n*-hexane in polyethylene between 25 and 120°C. The results obtained agreed with experimental data obtained at heating rates from 10 to 40°C/min up to 90°C and yielded an activation energy of 46 kJ/mol, which is in agreement with earlier reported experimental data.

Keywords: Thermogravimetry; Diffusion; Solute molecules; Numerical method

1. Introduction

Measurements of solute diffusivity have been performed almost exclusively at low temperatures when the polymer is in the solid state. The diffusion of molecules in polymers is however very different in the solid and the melt states and it is difficult to extrapolate diffusivity data beyond a polymer transition. It is important for several reasons to assess the diffusivity also at high temperatures. During processing/production of a packaging material, hot-filling of food into a polymer-based package or microwave heating of a food-containing package, it often happens that hazardous species enter or leave the polymer. In semi-virgin polymer films, the recycled layer may pollute the virgin layer during high-temperature lamination. It is also important to be able experimentally to determine diffusivities at high temperature for comparison with data obtained by molecular dynamics simulations. Thermogravimetry offers a possibility of obtaining diffusivity data over a wide temperature range from a single experiment. Miller and Wildnauer [1] derived a method for determining the diffusivity by using non-isothermal thermogravimetry and applying analytical expressions for sorption/desorption. This method was based on the idea that the desorption process can be represented during the heating scan by

* Corresponding author. Tel.: +46-8-790-76-40; fax: +46-8-790-69-46.
E-mail address: gedde@polymer.kth.se (U.W. Gedde)

0040-6031/00/$ – see front matter
PII: S0040-6031(00)00476-7

a series of isothermal states, each with a temperature slightly different from the previous state. The method is applicable only if the diffusivity is independent of solute concentration and if the process is diffusion-controlled. The time scale of the measurement must be large compared to the time required to achieve thermal equilibrium in the sample. The use of non-isothermal thermogravimetry for calculating pyrolysis kinetics has also been reported [2–5]. Hedenqvist et al. [6] used the Miller and Wildnauer method to measure the diffusivity of liquid propane in polyethylene.

In this paper, a more general treatment is presented for calculating the diffusivity of solute molecules in polymers over wide temperature ranges. The method is based on implicit numerical algorithms and is capable of treating the case of solute-concentration-dependent diffusivity. In addition, the method is combined with a thermal conductivity analysis in order to deal with fast heating conditions when thermal gradients exist within the specimen. The method is applied and tested on the desorption kinetics of *n*-hexane in polyethylene.

2. Experimental

The PE grade was an extrusion-coating grade (HE7541, Borealis AB, Sweden) with a density of 941 kg/m^3, a melting peak temperature of 130°C and a melt flow index of 7.5 g/10 min (ISO 1133). Samples with lateral dimensions of 10 mm×10 mm and a thickness of 630 μm were immersed in liquid *n*-hexane (purity 99%, Merck, density; ρ_1=656 kg/m^3) at 25°C and intermittently weighed until sorption equilibrium was attained. Prior to each weighing, the samples were surface dried. Isothermal and non-isothermal desorption measurements were performed on *n*-hexane-saturated samples using a Mettler–Toledo TGA-SDTA 851 thermogravimetric instrument. The samples were exposed to flowing nitrogen gas (50 ml/min) during the desorption.

3. Method for evaluation of desorption data obtained by TG

Fick's second law of diffusion for a plate specimen is given [7] by

$$\frac{\partial C}{\partial t} = \frac{\partial}{\partial x}\left(D(C,T)\frac{\partial C}{\partial x}\right) \tag{1}$$

where C is the penetrant concentration in g/cm^3. Only half the plate thickness was considered and the inner boundary co-ordinate is described as an isolated point:

$$\left(\frac{\partial C}{\partial x}\right)_{x=L} = 0 \tag{2}$$

The evaporative boundary conditions are described [8] by

$$D(C)\left[\frac{\partial C}{\partial x}\right]_{x=0} = F_0 C \tag{3}$$

where F_0 is the evaporation constant (cm/s) [8]. F_0 was taken to be large enough to avoid evaporation effects in the simulations. The isothermal diffusivity may be expressed [9] as

$$D(C) = D_{C0}\,\mathrm{e}^{\alpha C} \tag{4}$$

where D_{C0} is the zero-concentration diffusivity and α is a constant. The temperature dependence is conveniently described by the Arrhenius equation [7]:

$$D(C,T) = D_{CT0}\,\mathrm{e}^{\alpha(T)C}\,\mathrm{e}^{-\Delta E(C,T)/RT} \tag{5}$$

where D_{CT0} is the infinite temperature and zero concentration diffusivity and $\alpha(T)$ is temperature-dependent. Eq. (4) has been used extensively and it has been shown that it adequately describes isothermal diffusivity data [9]. It can be derived from the free volume theory [10]. In general, it is assumed that the temperature dependence of diffusion follows an Arrhenius type behaviour with an activation energy which is both concentration- and temperature-dependent ($\Delta E(C, T)$) [11]. By inserting Eq. (5) into Eq. (1) and discretising, the following expression is obtained:

$$\begin{aligned}\frac{\partial C}{\partial t} &= f(t,C,T)\\ &= \frac{D_{CT0}}{\Delta x_i^2}\Big(\mathrm{e}^{\alpha(T)C_{i+0.5}}\,\mathrm{e}^{-\Delta E(C_{i+0.5},T)/RT}(C_{i+1}-C_i)\\ &\quad -\mathrm{e}^{\alpha(T)C_{i-0.5}}\,\mathrm{e}^{-\Delta E(C_{i-0.5},T)/RT}(C_i-C_{i-1})\Big)\end{aligned} \tag{6}$$

where

$$C_{i\pm0.5} = \frac{C_i + C_{i\pm1}}{2} \tag{7}$$

Eq. (2) is best discretised using

$$C_{n+1} = C_{n-1} \tag{8}$$

Note that i=n at the centre of the plate. The surface boundary condition (i=0), given by Eq. (3), may be written as

$$C_0 = \frac{C_1}{1 + (\Delta x_i F_0)/(D_{CT0}\, e^{\alpha(T)C_1}\, e^{-\Delta E(C_1,T)/RT})} \tag{9}$$

In the case of non-isothermal desorption, it is more convenient to solve Eq. (1) as a function of temperature rather than of time:

$$\frac{\partial C}{\partial T} = \left(\frac{\partial T}{\partial t}\right)^{-1} \frac{\partial}{\partial x}\left(D(C,T)\frac{\partial C}{\partial x}\right) \tag{10}$$

where the term in the first bracket is the heating rate set by the thermogravimetrical instrument. If the diffusivity is analysed over a large temperature region which embraces both the solid and liquid (melt) states of the polymer, it is convenient to write Eq. (5) as

$$D(C,T) = \sum_{j=1}^{n} D_{CT0_j}\, e^{\alpha_j C}\, e^{-\Delta E_j/RT}\big|_{\Delta T_j} \tag{11}$$

where i refers to the temperature region ΔT_i. It is assumed that the temperature-dependence of α and the concentration- and temperature-dependence of ΔE is negligible within each region. n is the number of regions. Within a specific region, Eq. (6) together with Eqs. (10) and (11) may be expressed as

$$\frac{\partial C}{\partial T} = \left(\frac{\partial T}{\partial t}\right)^{-1} \frac{D_{CT0}}{\Delta x_i^2}\, e^{-\Delta E/RT} \times \left(e^{\alpha C_{i+0.5}}(C_{i+1} - C_i) - e^{\alpha C_{i-0.5}}(C_i - C_{i-1})\right) \tag{12}$$

The concentration profiles were generated using the following implicit multi-step relationship (m is the time co-ordinate):

$$\nabla^3 C_{m+1} = \frac{6}{11}\Delta t_m \left(f(t_{m+1}, \nabla^3 C_{m+1} + \nabla^2 C_m + \nabla C_m + C_m) - \frac{1}{\Delta t_m}\left(\frac{3}{2}\nabla^2 C_m + \nabla C_m\right)\right) \tag{13}$$

The details of the method are described by Hedenqvist et al. [9]. The implicit method integrates with respect to time using arcs with three constant time steps but with a variable step-size between them. The first arc was produced by a three-stage second-order Runge–Kutta method. The concentration profiles were integrated using Simpson's method with the Romberg routine to obtain higher accuracy. The Jacobian matrix needed for the multi-step method was calculated from Eqs. (14)–(16):

$$\frac{\partial f(T,C)}{\partial C_{i-1}} = \frac{D_{CT0}\, e^{-\Delta E/RT}}{\Delta x_i^2} \times \left(e^{\alpha C_{i-0.5}} - \frac{\alpha}{2} e^{\alpha C_{i-0.5}}(C_i - C_{i-1})\right) \tag{14}$$

$$\frac{\partial f(T,C)}{\partial C_i} = \frac{D_{CT0}\, e^{-\Delta E/RT}}{\Delta x_i^2}\left(\frac{\alpha}{2} e^{\alpha C_{i+0.5}}(C_{i+1} - C_i) - e^{\alpha C_{i+0.5}} - \frac{\alpha}{2} e^{\alpha C_{i-0.5}}(C_i - C_{i-1}) - e^{\alpha C_{i-0.5}}\right) \tag{15}$$

$$\frac{\partial f(T,C)}{\partial C_{i+1}} = \frac{D_{CT0}\, e^{-\Delta E/RT}}{\Delta x_i^2} \times \left(\frac{\alpha}{2} e^{\alpha C_{i+0.5}}(C_{i+1} - C_i) + e^{\alpha C_{i+0.5}}\right) \tag{16}$$

In order to take temperature gradients in the thickness direction into account, the heat equation:

$$\frac{\partial T}{\partial t} = \frac{1}{\rho(T)C_p(T)}\frac{\partial}{\partial x}\left(k(T)\frac{\partial T}{\partial x}\right) \tag{17}$$

was combined with the multi-step method Eq. (13) and discretised in the same manner as in Eq. (12) to give

$$\frac{\partial T}{\partial t} = \frac{1}{\Delta x_i^2}\left(\frac{k(T_{i+0.5})}{\rho(T_{i+0.5})C_p(T_{i+0.5})}(C_{i+1} - C_i) - \frac{k(T_{i-0.5})}{\rho(T_{i-0.5})C_p(T_{i-0.5})}(C_i - C_{i-1})\right) \tag{18}$$

where $\rho(T)$ and $C_p(T)$ are the density and heat capacity and $k(T)$ is the thermal conductivity. The surface boundary conditions are given by

$$T_{m+1} - T_m = \left(\frac{\partial T}{\partial t}\right)(t_m - t_{m-1}) \tag{19}$$

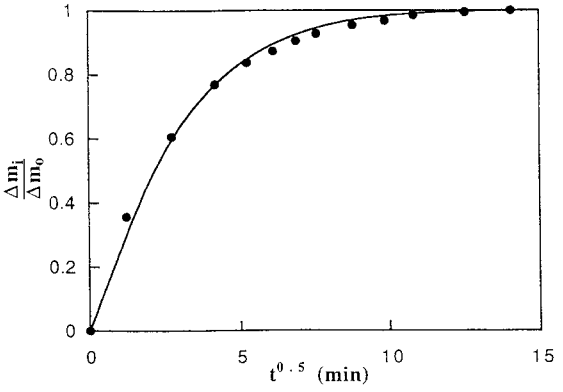

Fig. 1. Experimental *n*-hexane desorption data obtained at 30°C (●). The best fit of the numerical equations is given by the solid line.

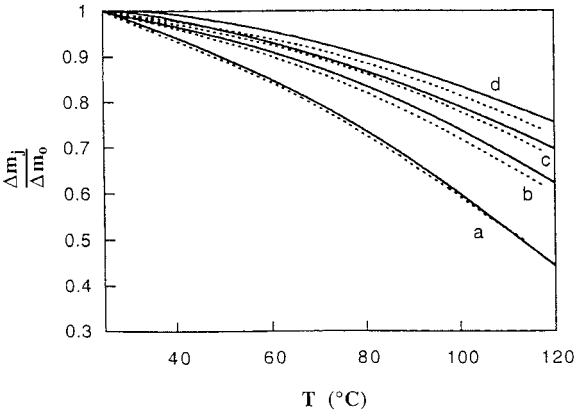

Fig. 2. Non-isothermal desorption curves. Solid and dotted lines are experimental and fitted curves, respectively. The heating rates are: (a) 10°C/min; (b) 20°C/min; (c) 30°C/min and (d) 40°C/min. Temperature gradients within the sample are neglected in this case.

where the term in the brackets is the heating rate set by the thermogravimeter.

3.1. Results and discussion

The method was tested on polyethylene at temperatures between 25 and 120°C. To obtain the zero-concentration diffusivity and the solute-concentration dependence (α), isothermal desorption was carried out at 30°C (Fig. 1). The saturation concentration of *n*-hexane at 30°C was 3.89 wt.% and $D_{C0}=2\times10^{-8}$ cm^2/s and $\alpha=80$ (wt.%)$^{-1}$. The zero-concentration diffusivity of *n*-hexane obtained is close to earlier reported values on low-density polyethylene at 25°C ($1.05–1.35\times10^{-8}$ cm^2/s) [12,13].

The isothermal parameters, D_{C0} and α, were inserted into Eq. (5) to fit the non-isothermal data obtained at different heating rates: 10–40°C/min (Fig. 2). In all the calculations of the non-isothermal cases, it was assumed that the thermal conductivity in the surrounding gas was sufficient to eliminate any temperature gradients between the oven walls and the specimen surface. This assumption was confirmed by inserting the proper thermal kinetics data of the gas into Eq. (17) and calculating the temperature profiles in the surrounding atmosphere. Fig. 2 shows that the fits were surprisingly good, considering that no thermal corrections were included. The numerical method was, thus, capable of describing the effects of heating rate on the desorption curve. However, a small deviation occurred at the highest heating rate (40°C/min), which indicates that the heat transport within the specimen has to be considered for this particular case. From the fits it was possible to calculate the activation energy of diffusion: 32.5 kJ/mol ($D_{C\!T0}=8\times10^{-3}$ cm^2/s). This is lower than earlier reported data (45.5–55.4 kJ/mol) [12,13], a fact which substantiates the argument that the thermal gradient has to be considered.

Possible thermal gradient effects were considered as follows: first the average temperature in the sample was calculated as a function of time during heating. Secondly, the non-isothermal experimental data were shifted along the temperature axis towards lower temperatures corresponding to the average temperature in the specimen during the heating scan. Thirdly, the non-isothermal data were fitted by Eqs. (10)–(16). In order to use Eq. (17), the temperature dependence of the parameters in the equation had to be determined. The thermal conductivity $k(T)$ according to data of Eierman [14] was: $k(T)=0.3871–0.00074T$ (J/m K s), and the heat capacity according to Gauer and Wunderlich [15] was: $C_p(T)=1595+7.64T$ (J/kg K). The density–temperature relationship was estimated from data of Olabisi and Simha [16] on linear polyethylene: $\rho(T)=951–0.4T$ (kg/m^3). Observe that the temperature in the three relationships above should be in °C. It was assumed that these parameters obeyed a

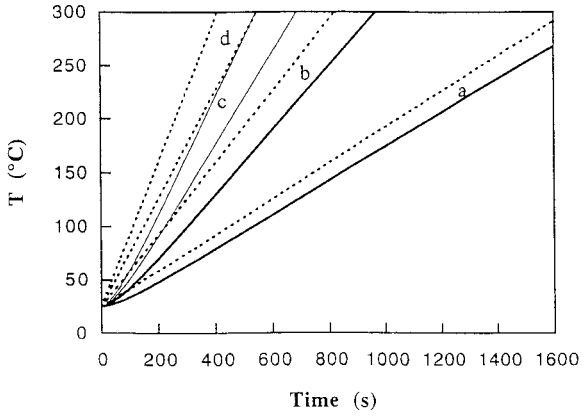

Fig. 3. Average temperature within a plate sample as a function of time according to Eq. (17). The heating rates are as follows: (a) 10°C/min; (b) 20°C/min; (c) 30°C/min and (d) 40°C/min. The dotted line is for infinite thermal conductivity and the solid line is calculated based on Eqs. (17)–(19).

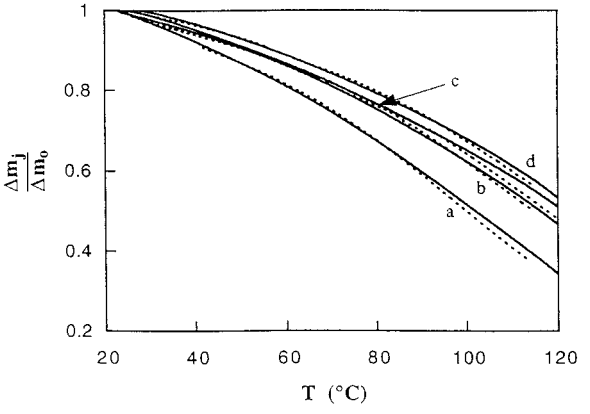

Fig. 5. Non-isothermal desorption curves with corrections for heat transfer within the specimen. Solid and dotted lines are shifted experimental data and corresponding fittings using Eqs. (10)–(16). The heating rates are: (a) 10°C/min; (b) 20°C/min; (c) 30°C/min and (d) 40°C/min.

linear temperature dependence within the considered temperature range (25–120°C). The thermal diffusivity ($k(T)/\rho(T)C_p(T)$) decreased by 30% from 25 to 90°C. Fig. 3 displays the average specimen temperature at different heating rates with infinite and finite thermal conductivity calculated from Eqs. (17)–(19). Fig. 4 illustrates the calculated temperature profiles (Eqs. (17–19)) along the thickness of the plate specimen at 40°C/min. The maximum difference between the surface and the core is about 40°C. Fig. 5 shows the shifted experimental non-isothermal desorption data and the corresponding fitted curves based on Eqs. (10)–(16). The agreement between fitted and experimental data is better than for the case displayed in Fig. 2. There is still a slight deviation at higher temperatures, presumably due to partial melting of the polymer. The calculated activation energy of diffusion was 46 kJ/mol, which is in good agreement with earlier reported data based on isothermal experiments [12,13].

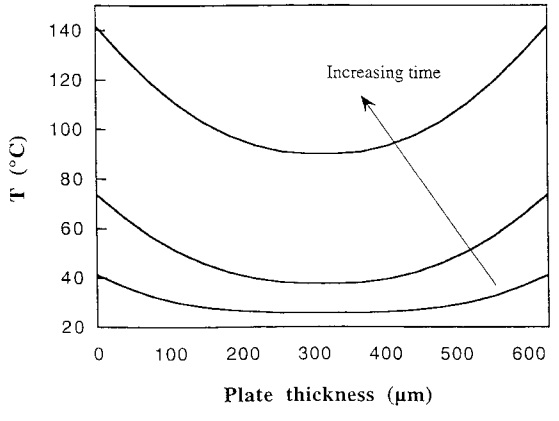

Fig. 4. Calculated temperature gradients along the thickness of the polymer using Eqs. (17) and (20)–(22) at 40°C/min.

The non-isothermal technique combined with the heat transfer equation has several advantages compared to the analytical non-isothermal techniques presented earlier [1]: It makes possible a rapid and accurate determination of the activation energy, and the concentration dependence of diffusivity can be taken into account. As a result of the combination with heat transfer the condition of thermal equilibrium in the specimen during the heating scan need not be fulfilled. This enables the use of high heating rates and thick specimens. The possibility of using thick specimens is particularly favourable because the accuracy of the measurement increases with increasing specimen thickness. The present technique also allows for the use of a thermal diffusivity which is temperature-dependent. Additionally, by a rigorous non-linear optimisation, i.e. by the use of a simplex search algorithm, it should be possible to determine the solute diffusion and thermal conductivity parameters with non-isothermal desorption by varying both sample thickness and heating rate.

4. Conclusions

It has been shown that the numerical non-isothermal thermogravimetric method is capable of describing solute diffusivity over large temperature regions, especially when it is combined with heat transfer equations. It accurately described the effects of variations in heating rates. It is superior to analytical non-isothermal methods in that it is fast and that it is not necessary to maintain thermal equilibrium in the specimen. It is possible by this method to include concentration-dependent solute diffusivity and temperature-dependent thermal diffusivity.

5. Nomenclature

α	constant describing the magnitude of the concentration dependence
C	solute concentration
D	diffusion coefficient
D_{C0}	diffusion coefficient at zero solute concentration
D_{CT0}	diffusion coefficient at zero solute concentration and zero temperature
ΔE	activation energy of diffusion
m	integral number of the time position
Δm_i	m_0–m_t
Δm_j	m_t–m_∞
Δm_0	m_0–m_∞
m_t	mass loss at time t
m_0	initial mass
m_∞	mass of dry polymer
F_0	rate of evaporation
C_p	heat capacity
i	integral number of the spatial position along x
j	integral number of the region
k	thermal conductivity
l	plate thickness
L	thickness of half of the plate
n	number of regions
R	the gas constant
ρ_1	solute density
ρ_2	polymer density
T	temperature
t	time

Acknowledgements

This study has been sponsored by the Swedish Research Council of Engineering Sciences (TFR; Grant: 97–125 doss 210) and the National Graduate School in Scientific Computing (NGSSC; Grant: 200–97–24).

References

[1] D.L. Miller, R.H. Wildnauer, Thermochim. Acta 14 (1976) 151.
[2] C.D. Doyle, J. Appl. Polym. Sci. 5 (1961) 285.
[3] C.D. Doyle, J. Appl. Polym. Sci. 6 (1962) 639.
[4] A. Broido, J. Polym. Sci. Polym. Phys. 7 (1969) 1761.
[5] T. Ozawa, J. Therm. Anal. 5 (1973) 563.
[6] M. Hedenqvist, T. Tränkner, A. Varkalis, G. Johnsson, U.W. Gedde, Thermochim. Acta 214 (1993) 111.
[7] J. Crank, The Mathematics of Diffusion, Clarendon Press, Oxford, 1986.
[8] A. Bakhouya, A.E. Brouzi, J. Bouzon, J.M. Vergnaud, Plast. Rubber Comp. Proc. Appl. 19 (1993) 77.
[9] M.S. Hedenqvist, U.W. Gedde, Polymer (1999).
[10] M.S. Hedenqvist, A. Angelstok, L. Edsberg, P.T. Larsson, U.W. Gedde, Polymer 37 (1996).
[11] M. Hedenqvist, U.W. Gedde, Progr. Polym. Sci. 21 (1996) 299.
[12] M. Fels, R.Y.M. Huang, J. Appl. Polym. Sci. (1970) 523.
[13] O.T. Aboul-Nasr, R.Y.M. Young, J. Appl. Polym. Sci. 23 (1979) 1819.
[14] K. Eierman, Kolloid Z. 201 (1965) 3.
[15] U. Gaur, B. Wunderlich, J. Phys. Chem. 10 (1981) 119.
[16] O. Olabisi, R. Simha, Macromolecules 8 (1975) 206.